

Journal of Materials and Engineering Structures

Research Paper

Finite Element Analysis of RC Beams Retrofitted and Strengthened with CFRP

Muhammad Azeem [a], Muhammad Fahim [b], Fasih Ahmed Khan [a], Muhammad Haris [a,*]

[a]*University of Engineering and Technology, Peshawar, Pakistan.*

[b]*Department of Civil Engineering, University of Engineering and Technology, Peshawar, Pakistan*

ARTICLE INFO

Article history :

Received 21 August 2023

Revised 18 February 2024

Accepted 23 March 2024

Keywords:

Finite element modelling,

CFRP

Retrofitting

Strengthening

Load-deflection behavior

ABSTRACT

This study aims to develop a finite element model for accurately predicting the behavior of RC beams retrofitted and strengthened with CFRP strips. Two types of CFRP layout are modelled, CFRP wraps at the bottom without any anchorage, and CFRP strips with CFRP wrap as anchorage. The developed numerical models are validated by experimentally testing RC beam models for four-point bending. The concrete damage plasticity model is used for introducing non-linearity in concrete. The non-linear tensile and compressive parameters are taken from the ABAQUS manual specifications. The interface between the CFRP and RC beam surface was replicated using a perfect bond between the two. The results show that the developed numerical model accurately predicts the strength of retrofitted and strengthened beams. Though numerical models show higher initial stiffnesses and cracking load, especially in the case of a retrofitted specimen, where the initial stiffness is as high as 75%.

1 Introduction

Fibre-reinforced polymers (FRP) have shown great potential in modern civil engineering applications owing to their durability, tensile strength and the strength-to-weight ratio [1, 2]. Its applications include strengthening reinforced concrete (RC) beams, columns, and slabs and increasing load bearing capacity of existing shear walls. FRP are primarily categorized into synthetic [3, 4] and natural fibres [5, 6]. The FRP external wraps are used for retrofitting and rehabilitation of existing bridges and buildings for strength enhancements [7, 8]. Synthetic fibres, in particular, are gaining interest for retrofitting and strengthening purposes. Carbon fibre-reinforced polymers (CFRP) have demonstrated great potential in the rehabilitation and strengthening of existing RC structures. When compared to traditional steel, CFRP has a unit weight between 1.5 and 1.6 g/cm^3, which is 5 times lighter [9]. Also, CFRP has a tensile strength that is 8 to 10 times greater than steel [2]. The application of CFRP strips on RC beams increases the flexural and shear capacity of the beam [10]. While CFRP wraps are

* *Corresponding author.*
E-mail address: harishussain75@gmail.com

e-ISSN: 2170-127X, (cc) BY-SA

RESEARCH REVIEW of Sciences and Technologies

also quite effective for strengthening beams against torsion [11]. Anchorage of CFRP with or without mechanical anchors plays a significant role in the behavior of retrofitted elements. Li et al. [12] compared the behavior of eight RC cantilever beams strengthened with CFRP laminate. It was concluded from the study that the bottom bonding and side bonding of RC beams with CFRP laminate significantly improve the flexural strength and stiffness. Additionally, the anchoring phenomena affects the fracture width and raises the pre-cracking load. [13].

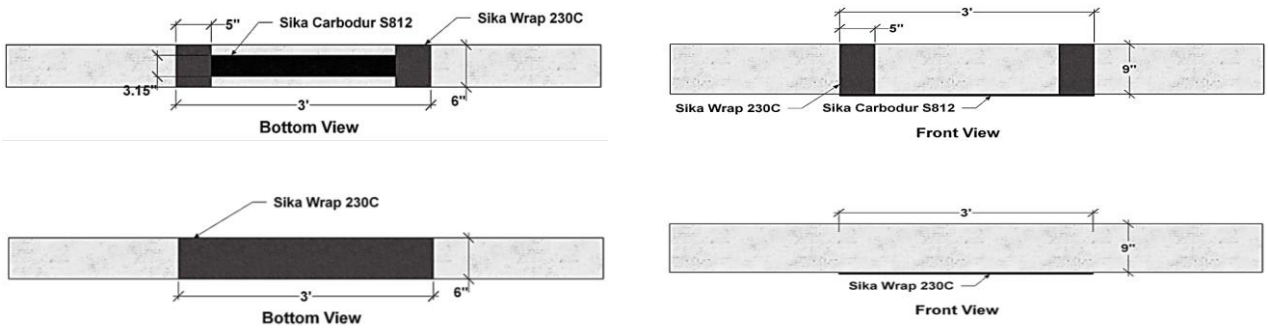
Several studies have been performed on developing numerical models for the assessment of concrete structures. ABAQUS/CAE is a finite element software, which is used extensively for the analysis of complex problems. In ABAQUS, two techniques for forecasting concrete behavior are the concrete damage plasticity (CDP) model and smeared cracking model. For this study concrete damage plasticity model was selected for modelling concrete since it has a higher convergence than that of the smeared crack model. The two primary failure mechanisms of concrete are crushing and cracking as per the concrete plastic damage model [14]. CDP introduce nonlinearity in concrete by combining the elastic behavior of concrete with compressive and tensile plasticity [15] and [16].

One of the challenging aspects of numerical modelling of CFRP retrofitted RC beams is to establish an interface between the CFRP and concrete surface. Several studies have been performed on the CFRP and concrete surface interface for dynamic behavior. Yuan et al. [17] carried out a single lap test to examine the bond behavior between concrete and CFRP sheet under various loading. The authors concluded that the CFRP sheet and concrete interface bond are sensitive to strain rate and debonding of the CFRP-concrete interface is the governing failure mode. By adding the strain rate effect, Yuan et al. [18] also proposed a 3D numerical model of the interface between FRP and concrete. Furthermore, the semiempirical model is presented to incorporate the dynamic increase factor and strain rate to forecast the debonding load and ultimate debonding strain.

This research aims to develop a finite element numerical model for strength prediction of RC beams retrofitted and strengthened with CFRP. Finite element-based software ABAQUS is used for developing the RC beams models. The results from numerical modelling are also validated by experimental testing of RC beams.

2 Experimental Program

In this research, five reinforced concrete beam models were tested. One of the five specimens was a control beam with no retrofitting denoted as “B1-CB”. Two types of CFRP were used in this study for strengthening and retrofitting, stirp type (Sika Carbodur S812) and sheet type (Sika Wrap 230C), specifications of which are summarized in Table 1. Two arrangements of CFRP were used for strengthening as shown in Fig. 1. The first pattern had a 3.15-inch wide and 0.0394-inch thick strip, anchored with 5-inch wide U-shaped strips at the ends. The second pattern had a 6-inch wide and 0.0052-inch thick wrap. No U-shaped anchorage was applied in this pattern. These two strengthened specimens were denoted as “S1-CD” and “S2-SW”, respectively. The remaining two specimens were tested to cracking load initially without CFRP. The tested cracked specimens were then retrofitted using a similar layout as strengthened models as shown in Fig. 1 and were tested to collapse. The two retrofitted specimens were denoted as “R1-CD” and “R2-SW”.



(a) **(b)**

Fig. 1 – CFRP layout for (a): S1-CD and R1-CD, (b): S2-SW and R2-SW specimens

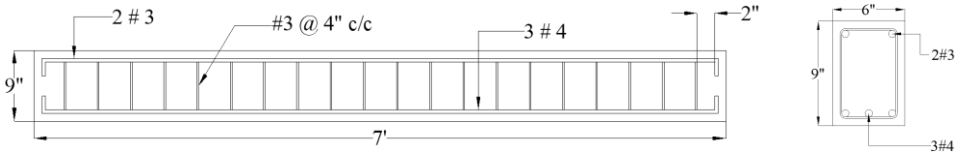


Fig. 2 – Reinforcement layout of the test specimens

Table 1 – Material Specifications

CFRP Type	Width (in)	Thickness (in)	Strength (ksi)	Modulus of Elasticity (ksi)
Sika Carbodur S812	3.15	0.047	400	23.2×10^3
Sika Wrap 230C	6	0.0052	460	31.9×10^3
Concrete	-	-	4	3604
Steel Grade 60	-	-	60	29.0×10^3
Steel Grade 40	-	-	40	29.0×10^3

It is worth mentioning here that the geometry and reinforcement details for all the beam specimens designed according to ACI-318 are kept the same as shown in Fig. 2. Concrete with a specified compressive strength of 4,000 psi was used for the fabrication of specimens. The representative concrete cylinders from each batch were tested under ASTM C39. The average compressive strength of concrete cylinders was 3,940 psi. For longitudinal and transverse reinforcement, ASTM A615 Grade 60 and Grade 40 steel were used respectively. The average yield strength of Grade 60 and Grade 40 steel tested under ASTM, was 59.94 ksi and 52.24 ksi respectively.

All the specimens were subjected to a 4-points bending test. The test setup for this arrangement is shown in Fig. 3. The vertical load was applied through a vertical load cell of 50 tons capacity. Three linear variable displacement transducers (LVDTs) were used to capture the deflection of the beam at mid-span and one-third of the span as shown in Fig. 3.

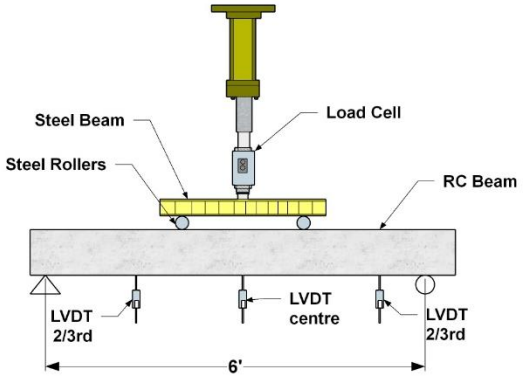


Fig. 3 – Typical test setup for four-point bending test

3 Finite Element Model

The finite element analysis for this study was carried out in ABAQUS/CAE version 6.14. Three-dimensional FE models of RC beams were created based on the main goals of this study, and the different aspects of modeling are discussed below.

Three primary materials concrete, steel, and CFRP are modeled in this study. CPD model is used to model the behavior of concrete as discussed in section 3.1.1. Elastic perfectly plastic beahaviour is used to model the steel reinforcement. The CFRP material is assumed to perfectly elastic. Static general analysis type was selected in the step module to carry out the analysis. Embedded region constraint was used to embed the reinforcement bars in the concrete beam and Tie constraint is used to define the perfect bond behavior between the CFRP strips and concrete beam. Tie constraint allow to fuse together

two regions. Pin and roller supports was used to define the boundary condition. A 3D Solid element was used for the modelling of parts. We used an 8-node continuum solid element (C3D8R) to develop the concrete beam and 2-node linear truss element (T3D2) is used to develop the reinforcement bars. All of these elements have three degrees of freedom in each node. Global seed size of 2.09 was used for meshing with total of 1125 nodes as shown in Figure 7.

3.1 Material Models

The materials used for the fabrication of the model consist of concrete, steel and CFRP. In recent decades, many constitutive models have been developed that may simulate concrete behavior, involving crushing and fractures. In ABAQUS, two techniques for forecasting concrete behavior are the Plastic Damage model and smeared cracking model. For the study Plastic Damage was selected since it has a higher convergence than that of the smeared crack model. The two primary failure mechanisms of concrete are crushing and cracking as per the concrete plastic damage model [14].

3.1.1 The concrete damage plasticity model

The concrete damage plasticity (CDP) approach was used for the modelling of concrete. CDP is recommended model for the analysis of concrete, bricks and other quasi-brittle material under monotonic and dynamic loading. CDP introduce nonlinearity in concrete by combining the elastic behavior of concrete with compressive and tensile plasticity [15] and [16]. The elastic and non-elastic behavior of this model both in tension and compression is demonstrated in Fig. 4. The concrete was modelled as a solid, homogenous material and the elastic properties of concrete are summarized in Table 2.

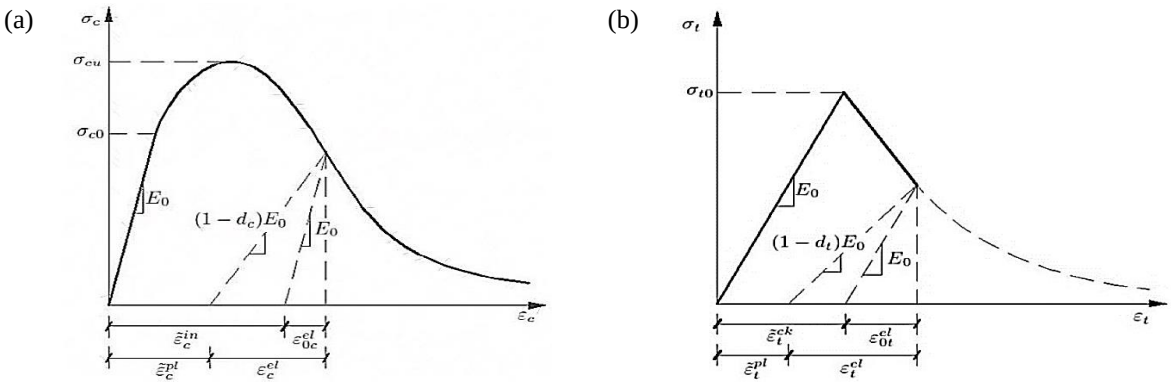


Fig. 4 – Damage response to inelastic (a): Compression, (b): Tension [19]

Table 2 – Elastic properties of concrete

Parameters	Specified Values
Density	145 (lb/ft3)
Poisson's ratio	0.16
Elastic Modulus	3600 ksi

Table 3 – Concrete damage plasticity parameters

Parameters	Dilation Angle	Eccentricity	Fb0/fc0	K	Viscosity Parameter
Values	31	0.1	1.16	0.67	0.003

To define the non-linear plastic behavior of concrete, the plasticity parameters were taken from the ABAQUS manual [20], which is summarized in Table 3. In the CDP model, the inelastic compressive properties are defined by inelastic strains and the inelastic tensile behavior by cracking stains. The inelastic and cracking strains can be calculated using equation (1).

$$\varepsilon_{in,cr} = \varepsilon_t - \varepsilon_{el} \tag{1}$$

Where ε_t and ε_{el} represent total and elastic strains respectively. These values are taken from the ABAQUS manual and are specified in Fig. 5. To idealize the damage in material beyond the peak load, the damage parameter (dc) is used, which can be calculated using equation (2).

$$d_{c,t} = 1 - \frac{\sigma_{c,t}}{\sigma'_{c,t}} \tag{2}$$

Where dc is the damage parameter after peak, σ represents the corresponding strengths σ' is the ultimate strength. The plastic strain can be calculated using equation (3).

$$\varepsilon_{pl_{c,t}} = \varepsilon_{in_{c,t}} - \frac{d_{c,t}}{1-d_{c,t}} \cdot \frac{\sigma_{c,t}}{E_o} \tag{3}$$

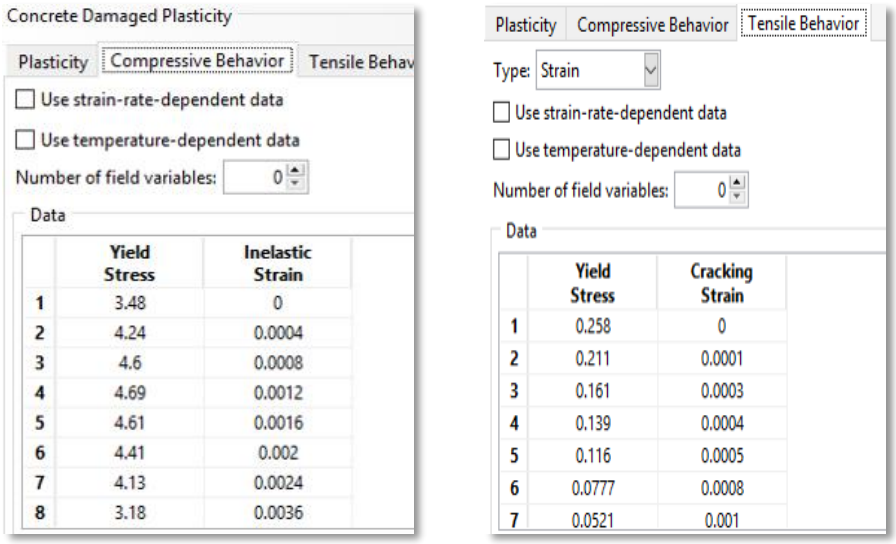


Fig. 5 – Defining inelastic compressive (left) and tensile (right) properties

3.1.2 Material Models for Steel and CFRP

An elastic perfectly plastic model has been used to simulate the constitutive characteristics of steel with the same properties in compression and tension. Two different grades of steel were used in this study for longitudinal (60 ksi) and transverse reinforcement (40 ksi). The steel elements were defined as isotropic and elastic materials. The Young's modulus and the poisons ratio were set to standard values of 29000 ksi and 0.3 respectively. Plastic properties of steel such as, hardening is Isotropic, number of field variables are set equal to zero to ignore the plastic behavior. Young's modulus was set to 60 ksi and 40 ksi for grade 60 and 40 steel, respectively.

The CFRP material is considered to be linear elastic isotropic until rupture in this study. For the CFRP, there is no considerable difference between the orthotropic and elastic isotropic models [21]. The unidirectional Sika Carbodur S812 CFRP material had a 23200 ksi modulus of elasticity in the direction of fibres; While Sika Wrap 230C used in the testing had a 34518 ksi modulus of elasticity in the direction of fibres and a poison ratio of 0.3, according to the manufacturer. The above values of v = 0.3 and E are used in the CFRP material modelling.

3.2 Modelling approach in ABAQUS

The elements are modelled in the part module of ABAQUS. The concrete beam was modelled as a 3D deformable element C3D8R, while the longitudinal bars and stirrups are modelled as a T3D2 element. The properties are assigned to created parts from the material module. The parts are then assembled in the assembly module. The interfaces between steel-concrete and concrete-CFRP were simulated as perfect bonds. Concentrated static loads were applied in the vertical direction corresponding to the experimental tested models as shown in Fig. 6. Meshing plays an important role in the FEA. Decreasing

mesh size in the FEA model improves the preciseness of results while also increasing the time it takes to solve the equations [22]. The meshed beam model is shown in Fig. 7.

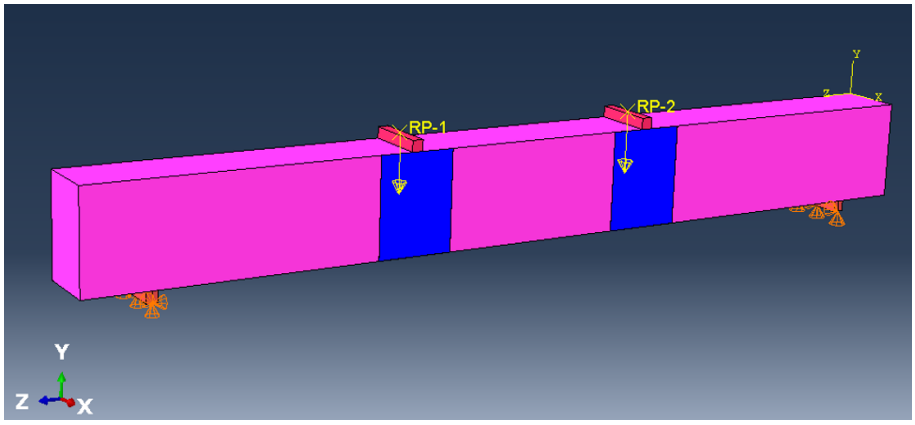


Fig. 6 – Beam model after load assignment

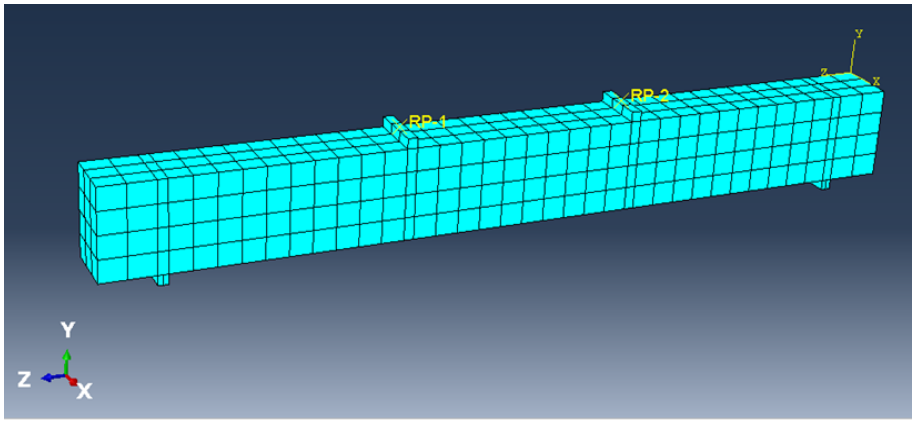


Fig. 7 – FE Meshing of concrete beam specimen

4 Results and Discussion

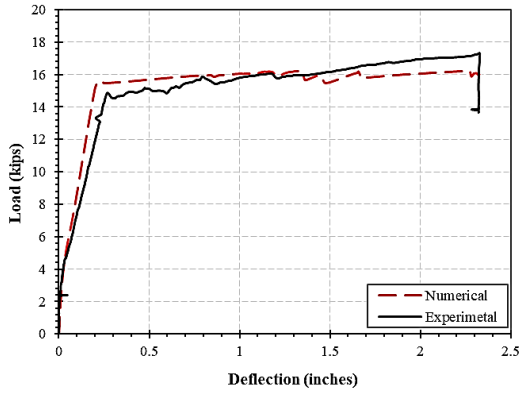
4.1 Load-Displacement specimen response

The load-displacement curves obtained through finite element analysis and the corresponding experimental curves for each specimen are shown in Fig. 8. The maximum loads and displacements of each specimen are summarized in

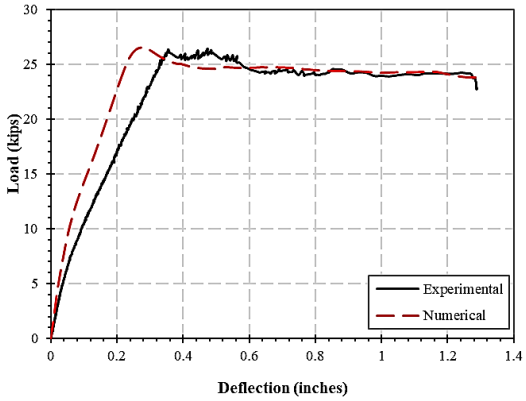
. The control beam “CB” was used to validate the finite element model. The numerical load-deflection curve of the control beam is in close agreement with experimental values. The numerical peak load shows a slightly conservative value as compared to the numerical peak load.

The difference between the stiffness of numerical and experimental models in linear range and after cracking is summarized in Table 5. In the case of the control beam, the initial stiffness of FEM analysis matches nicely with the experimental model. A slight difference is noted in the stiffness after the cracking of the specimen.

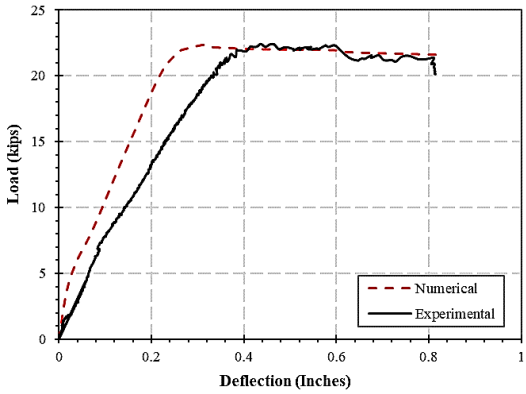
The FEM provide a very reliable model for a maximum load of retrofitted and strengthened specimens as shown in table 4. However, numerical models demonstrate quite higher initial stiffness for all specimens. The difference in stiffness of numerical and experimental specimens is relatively less after the initial cracking.



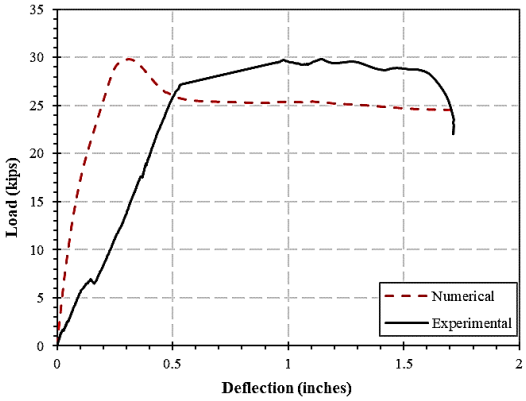
(a) Specimen B1-CB experimental and numerical load-deflection curves



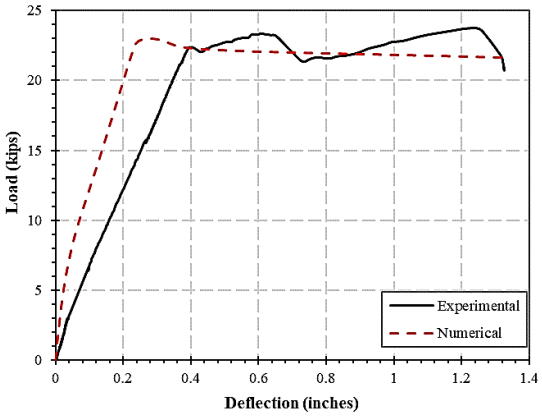
(b) Specimen S1-CD experimental and numerical load-deflection curves



(c) Specimen S2-SW experimental and numerical load-deflection curves



(d) Specimen R1-CD experimental and numerical load-deflection curves



(e) Specimen R2-SW experimental and numerical load-deflection curves

Fig. 8 – Experimental and numerical load-deflection curves of all specimens

The load-deflection curves of all the specimens are shown in Fig. 9. The control beams were tested initially up to cracking, without any CFRP. The cracked beams were retrofitted as discussed earlier. It can be observed from the load-deflection curve that the beam retrofitted with CFRP strips and U-shaped anchors regained its original strength, while the beam retrofitted with only CFRP wrap without anchorage only regain some portion of its strength. In both cases, higher ultimate displacement was noted in retrofitted specimens, however, stiffness was reduced in both cases. The stiffness reduction was much more obvious in the specimen retrofitted with CFRP wrap. A similar pattern to retrofitted specimens

was also noted in beams strengthened from the start. The beam strengthened with CFRP strip and U-shaped anchored had the highest strength of all the specimens.

Table 4 – Maximum loads and deflection in each specimen

Beam ID	Maximum Deflection (in)	Maximum Load		
		Numerical (kips)	Experimental (kips)	% difference
B1-CB	2.33	16.22	17.3	6.24
S1-CD	1.29	26.52	26.43	0.36
S2-SW	0.81	22.36	22.43	0.31
R1-CD	1.72	29.81	29.83	0.03
R2-SW	1.33	23.59	23.72	0.55

Table 5 – Difference between numerical and experimental stiffness

Beam ID	Stiffness Difference	
	In Linear Range (%)	After Initial Cracking (%)
B1-CB	0%	29%
S1-CD	37%	17%
S2-SW	54%	31%
R1-CD	75%	40%
R2-SW	59%	35%

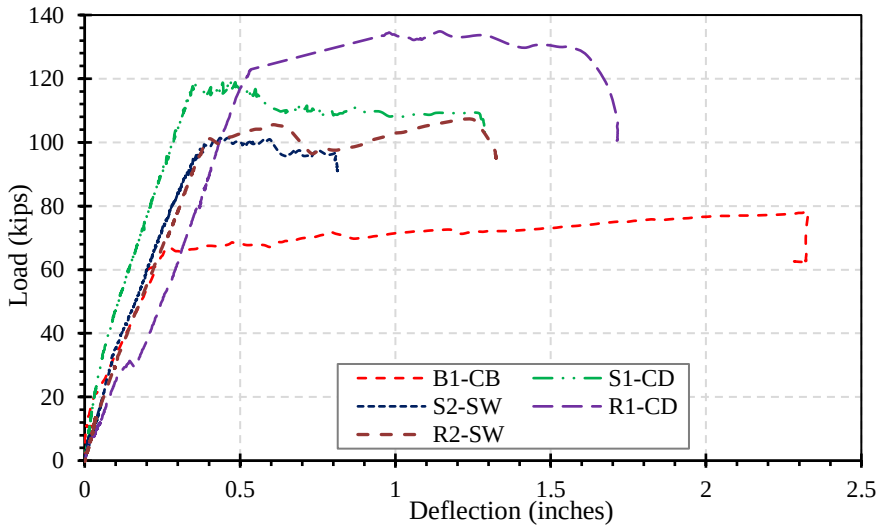


Fig. 9 – Load-Displacement graphs of center gauges for all specimens

4.2 Cracking load and failure pattern

The initial cracking load of all specimens are specified in Table 6. The predominant failure mode in the retrofitted and strengthened specimen was the debonding of CFRP strips from the concrete. The maximum strains demonstrated by numerical specimens are shown in Fig. 10 and the final damage pattern of all tested specimens is shown in Fig. 11. All the specimens demonstrated predominant tensile cracking in the lower face of the beam due to high tensile stresses in that region. The cracking was soon followed by debonding of CFRP from concrete due to the crack weakening the bond. The cracks were also affected by the type of CFRP layout. The U-shaped anchorage provided in S1-CD and R1-CD reduced the crack width. The debonding was also delayed in these specimens, as the U-shaped strip provided anchorage against premature debonding.

The specimens without any anchorage showed relatively wider concrete cracks and the debonding phenomenon was more obvious.

Table 6 – Experimental and numerical cracking load of all specimens

Initial Cracking Load			
Beam ID	**Numerical (kips)**	**Experimental (kips)**	**Error (%)**
B1-CB	**4.40**	4.40	**0**
S1-CD	**9.1**	7.71	**15**
S2-SW	**5.2**	6.82	**-30**
R1-CD	**12.14**	6.8	**42.9**
R2-SW	**6.21**	3.26	**47.5**

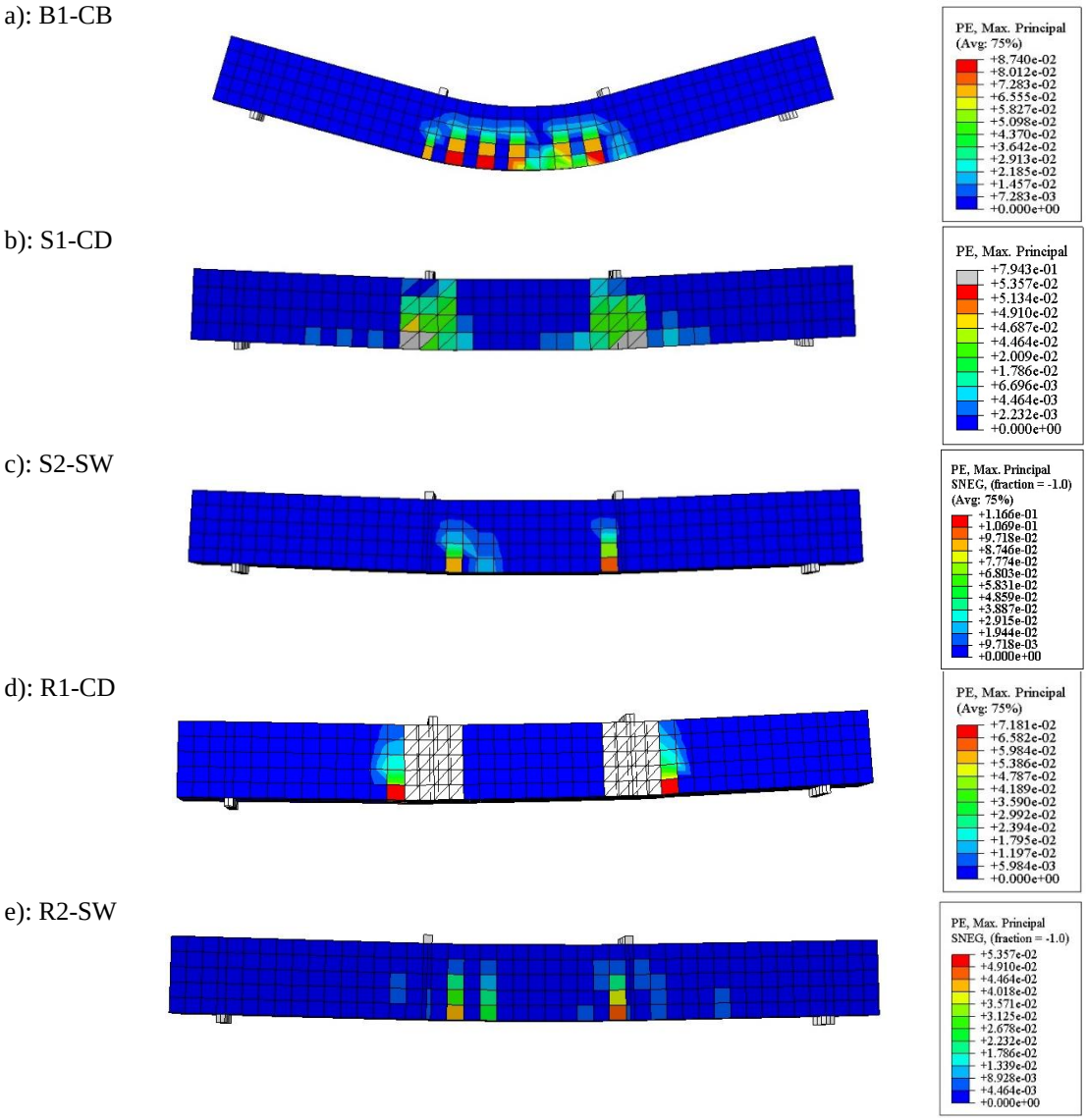


Fig. 10 – Maximum principal stains of each specimen

The numerically obtained initial cracking loads of the control and strengthened beam are relatively closer to experimental values as shown in Table 6. However, in retrofitted specimens, numerical analysis shows relatively higher values of initial crack loads. All the specimens demonstrated severe cracks in the centre lower face of the beam owing to high tensile stresses. The FEM models replicate the damage pattern of experimental behavior as shown in Fig. 11. Intense stress concentration can

be seen in the control beam, which was also verified by a huge concentrated crack at the midspan of the experimental tested model. The CFRP retrofitting assist in distributing the stresses on a larger area, hence a scattered crack pattern is noted in both strengthened and retrofitted specimens.

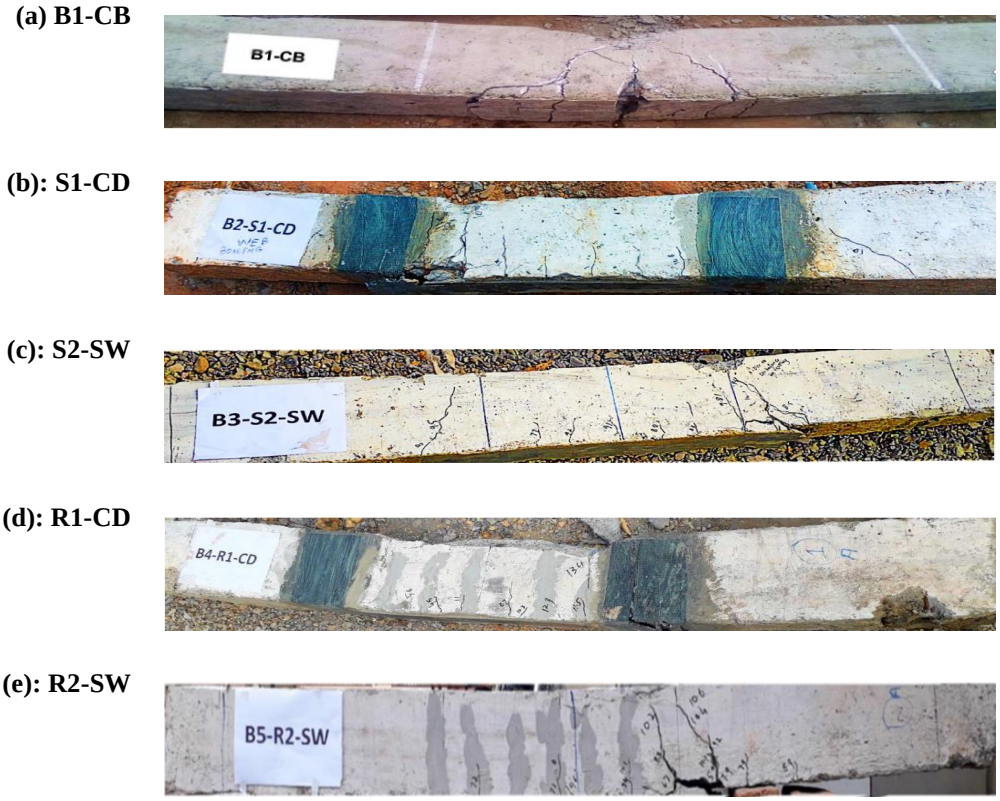


Fig. 11 – Damage pattern of experimentally tested specimens

5 Conclusions

This study was conducted to carry out finite element analysis of RC beams strengthened and retrofitted with CFRP. The numerical models were verified by experimental testing RC beams retrofitted and strengthened with CFRP for four points bending load. It is concluded from this study that

- The concrete damage plasticity model can predict the non-linear behavior of concrete through damage parameters.
- The strength and behavior of concrete beams strengthened and retrofitted with CFRP can be predicted by numerical modelling using the proper interface between CFRP strips and RC.
- The developed numerical model predicts slightly higher initial stiffness as compared to experimental models for all analysed specimens.
- The strengthening and retrofitting of RC beams with CFRP significantly increase the flexural strength of the beam.
- The numerical model demonstrated up to 45% higher initial cracking load in the case of retrofitted specimens.
- The anchorage of CFRP strips put a great emphasis on crack control. The U-shaped anchorage of the CFRP strip distributes the crack intensity evenly over a larger portion, hence forming smaller cracks as compared to the specimen without anchorage.
- Proposed numerical models can accurately predict the strength of CFRP retrofitted beams, which can be very helpful for the analysis and design of RC beams.

Declaration of competing interest

The authors declare that they have no known competing financial interests or personal relationships that could have appeared to influence the work reported in this paper.

REFERENCES

[1]- A. Siddika, M.A. Al Mamun, R. Alyousef, Y.M.J.J.o.B.E. Amran, Strengthening of reinforced concrete beams by using fiber-reinforced polymer composites: A review. 25 (2019) 100798.

[2]- M. Garcez, L. Meneghetti, L.C.J.J.o.C.f.C. da Silva Filho, Structural performance of RC beams poststrengthened with carbon, aramid, and glass FRP systems. 12(5) (2008) 522-530.

[3]- M.A. Karataş, H.J.D.T. Gökkaya, A review on machinability of carbon fiber reinforced polymer (CFRP) and glass fiber reinforced polymer (GFRP) composite materials. 14(4) (2018) 318-326.

[4]- H.A. Toutanji, M.J.S.J. Saafi, Flexural behavior of concrete beams reinforced with glass fiber-reinforced polymer (GFRP) bars. 97(5) (2000) 712-719.

[5]- M. Fahim, M. Haris, W. Khan, S.J.A.i.S. Zaman, T.R. Journal, Bamboo as a construction material: Prospects and challenges. 16(3) (2022) 165-175.

[6]- N. Sgriccia, M. Hawley, M.J.C.P.A.A.S. Misra, Manufacturing, Characterization of natural fiber surfaces and natural fiber composites. 39(10) (2008) 1632-1637.

[7]- S.A. Sheikh, M.T.J.A.S.J. Toklucu, Reinforced concrete columns confined by circular spirals and hoops. 90 (1993) 542-542.

[8]- P. Delgado, A. Arêde, N.V. Pouca, P. Rocha, A. Costa, R.J.C.S. Delgado, Retrofit of RC hollow piers with CFRP sheets. 94(4) (2012) 1280-1287.

[9]- C.E. Bakis, A. Ganjehlou, D.I. Kachlakev, M. Schupack, P. Balaguru, D.J. Gee, V.M. Karbhari, D.W. Scott, C.A. Ballinger, T.R.J.R.b.A.C. Gentry, Guide for the design and construction of externally bonded FRP systems for strengthening concrete structures. 440(2002) (2002).

[10]- S. Linwang, C. Jian, C. Qingjun, L. Guobao, Z.J.T.O.C.E.J. Juan, Investigation on the flexural behavior of corroded concrete beams repaired by CFRP sheet under different corrosion levels. 10(1) (2016).

[11]- M. Imran, N. Shafiq, I.J.A.M. Akbar, Materials, Strengthening Schemes for Flexure and Torsion using FRP Laminates: A State of Art Review. 567 (2014) 511-516.

[12]- G. Li, Y. Guo, X.J.T.O.C.E.J. Sun, Investigation on flexural performance of RC beams flexurally strengthened by side-bonded CFRP laminates. 6(1) (2012).

[13]- M. Fahim, F. Alam, H. Khan, I. Haq, S. Ullah, S.J.E. Zaman, Technology, A.S. Research, The Behavior of RC Beams Retrofitted with Carbon Fiber Reinforced Polymers (CFRP). 12(3) (2022) 8701-8706.

[14]- P. Grassl, M.J.I.j.o.s. Jirásek, structures, Damage-plastic model for concrete failure. 43(22-23) (2006) 7166-7196.

[15]- J. Lubliner, J. Oliver, S. Oller, E.J.I.J.o.s. Oñate, structures, A plastic-damage model for concrete. 25(3) (1989) 299-326.

[16]- J. Lee, G.L.J.J.o.e.m. Fenves, Plastic-damage model for cyclic loading of concrete structures. 124(8) (1998) 892-900.

[17]- C. Yuan, W. Chen, T.M. Pham, H. Hao, J. Cui, Y.J.I.J.o.A. Shi, Adhesives, Interfacial bond behaviour between hybrid carbon/basalt fibre composites and concrete under dynamic loading. 99 (2020) 102569.

[18]- C. Yuan, W. Chen, T.M. Pham, H. Li, H.J.C. Hao, B. Materials, Finite element modelling of dynamic bonding behaviours between fibre reinforced polymer sheet and concrete. 255 (2020) 118939.

[19]- J.B. Mander, M.J. Priestley, R. Park, Theoretical stress-strain model for confined concrete. Journal of structural engineeirng, 114(8) (1988) 1804-1826.

[20]- Hibbitt, Karlsson, Sorensen, ABAQUS: Theory manual. Vol. 2. Hibbitt, Karlsson & Sorensen, 1997.

[21]- S.K. Paul, P.J.I.R.J.o.E. Sahu, T. Volume, Finite element analysis of retrofitting of RC beam with CFRP using Abaqus. 7 (2020) 1268-1273.

[22]- Y. Liu, G.J.B.J.E.T. Glass, Choose the best element size to yield accurate FEA results while reduce FE model's complexity. 1 (2013) 13-28.